Plasmodium falciparum adapts its investment into replication *versus* transmission according to the host environment

Abdirahman I Abdi[1,2]*, Fiona Achcar[3,4], Lauriane Sollelis[3,4], João Luiz Silva-Filho[3,4], Kioko Mwikali[1], Michelle Muthui[1], Shaban Mwangi[1], Hannah W Kimingi[1], Benedict Orindi[1], Cheryl Andisi Kivisi[1,2], Manon Alkema[5], Amrita Chandrasekar[3], Peter C Bull[1], Philip Bejon[1], Katarzyna Modrzynska[3], Teun Bousema[5], Matthias Marti[3,4]*

[1]KEMRI-Wellcome Trust Research Programme, Kilifi, Kenya; [2]Pwani University Biosciences Research Centre, Pwani University, Kilifi, Kenya; [3]Wellcome Center for Integrative Parasitology, University of Glasgow, Glasgow, United Kingdom; [4]Institute of Parasitology, Vetsuisse and Medical Faculty, University of Zurich, Zurich, Switzerland; [5]Radboud University Nijmegen Medical Centre, Nijmegen, Netherlands

*For correspondence:
aabdi@kemri-wellcome.org
(AIA);
matthias.marti@glasgow.ac.uk
(MM)

Abstract The malaria parasite life cycle includes asexual replication in human blood, with a proportion of parasites differentiating to gametocytes required for transmission to mosquitoes. Commitment to differentiate into gametocytes, which is marked by activation of the parasite transcription factor *ap2-g*, is known to be influenced by host factors but a comprehensive model remains uncertain. Here, we analyze data from 828 children in Kilifi, Kenya with severe, uncomplicated, and asymptomatic malaria infection over 18 years of falling malaria transmission. We examine markers of host immunity and metabolism, and markers of parasite growth and transmission investment. We find that inflammatory responses associated with reduced plasma lysophosphatidylcholine levels are associated with markers of increased investment in parasite sexual reproduction (i.e. transmission investment) and reduced growth (i.e. asexual replication). This association becomes stronger with falling transmission and suggests that parasites can rapidly respond to the within-host environment, which in turn is subject to changing transmission.

Editor's evaluation

This important work provides insight into how *Plasmodium falciparum* optimises the balance between infection of the human host and investment in onward transmission to the mosquito. The results, based on appropriate and validated state-of-the-art methodologies, are convincing and have both theoretical and practical implications beyond a single subfield.

Introduction

Malaria remains one of the world's major public health problems. In 2021, an estimated 619,000 deaths and 247 million cases were reported (*WHO, 2022*). Around 70% of deaths are in African children under five years of age and are caused by a single parasite species, *Plasmodium falciparum* (*WHO, 2022*).

P. falciparum has a complex life cycle, involving obligatory transmission through a mosquito vector and asexual replication within erythrocytes of the human host. Between-host transmission requires the formation of gametocytes from asexual blood stage forms, as gametocytes are the only parasite stage to progress the cycle in the mosquito. A series of recent studies has demonstrated that commitment to gametocyte formation (i.e. stage conversion) is epigenetically regulated and occurs via activation of the transcription factor, AP2-G that in turn induces transcription of the first set of gametocyte genes (*Kafsack et al., 2014*; *Sinha et al., 2014*).

The parasites that do not convert into gametocytes continue to replicate asexually, contributing to within-host parasite population growth (i.e. parasite burden) and determining *P. falciparum* infection outcome that ranges from asymptomatic infections to severe complications and death (*Marsh and Snow, 1999*; *Langhorne et al., 2008*; *White, 2018*). Cytoadhesion of infected erythrocytes (IE) to receptors on microvascular endothelium of deep tissues reduces the rate of parasite elimination in the spleen (*Rowe et al., 2009*; *Turner et al., 2013*), thus supporting the within-host expansion of the parasite population (i.e. parasite burden). As a side effect of this parasite survival strategy, cytoadhesion reduces the diameter of the vascular lumen, thus impairing perfusion and contributing to severe malaria pathology (*Silamut et al., 1999*; *Taylor et al., 2004*; *Hanson et al., 2012*). *P. falciparum* erythrocyte membrane protein 1 (PfEMP1), encoded by the *var* multi-gene family, plays a critical role in both pathogenesis (through cytoadhesion) (*Smith et al., 1995*; *Su et al., 1995*) and establishment of chronic infection (through variant switching and immune evasion) (*Recker et al., 2004*; *Scherf et al., 2008*).

Both *var* gene transcription and stage conversion (and hence *ap2-g* transcription) are subject to within-host environmental pressures such as immunity (*Rono et al., 2018*), febrile temperature (*Oakley et al., 2007*; *Rawat et al., 2021*), nutritional stress (*Carter and Miller, 1979*), and drugs (*Buckling et al., 1999*), perhaps via a common epigenetic regulation mechanism (*Coleman et al., 2014*). For example, in vitro studies revealed that stage conversion can be induced by nutritional depletion such as spent culture media (*Carter and Miller, 1979*; *Williams, 1999*) and depletion of Lysophosphatidyl-choline (LPC) (*Brancucci et al., 2017*). Recent work from Kenya and Sudan provides some evidence that parasites in low relative to high transmission settings invest more in sexual commitment and less in replication and *vice versa* (*Rono et al., 2018*). Altogether these studies suggest that the parasite can sense and rapidly adapt to its environment in vitro and in vivo. A family of protein deacetylases called sirtuins is known to link environmental cues to various cellular processes via metabolic regulation (*Li, 2013*; *Bosch-Presegué and Vaquero, 2014*; *Vasquez et al., 2017*). They do this through epigenetic control of gene expression (*Vasquez et al., 2017*) and post-translational modification of protein function (*Vasquez et al., 2017*; *Zhu et al., 2012*). The *P. falciparum* genome contains two sirtuins (Pfsir2a/b) which have been linked to the control of *var* gene transcription (*Tonkin et al., 2009*; *Merrick et al., 2012*), and their expression is influenced by febrile temperature (*Oakley et al., 2007*) and low transmission intensity (*Rono et al., 2018*; *O'Meara et al., 2008*; *Mogeni et al., 2016*).

Here, we investigated the interplay between parasite and host environmental factors governing parasite investment in reproduction (to maximize between-host transmission) *versus* replication (to ensure within-host persistence) in vivo. We analyzed samples and clinical data collected from children in Kilifi county, Kenya, over changing malaria transmission intensity between 1994 and 2014. We quantified parasite transcripts for *ap2-g*, *PfSir2a,* and *var* genes, as well as *Pf*HRP2 protein levels (for parasite biomass) and levels of host inflammatory markers and lipid metabolites. We then integrated these host and parasite-derived parameters to interrogate their dynamics and interactions in the context of changing transmission intensity and immunity.

Results

A clinical malaria patient cohort across changing transmission periods in Kilifi, Kenya

The study included samples and clinical data collected from 828 children from Kilifi county, Kenya, over 18 years of changing malaria transmission (*O'Meara et al., 2008*; *Mogeni et al., 2016*). The study period encompassed three defined transmission phases: pre-decline (1990–2002), decline (2003–2008), and post-decline (2009–2014) (*Figure 1A*). During the study period, a total of 26,564 malaria admissions were recorded at Kilifi county hospital (*Figure 1A and B*). While the number
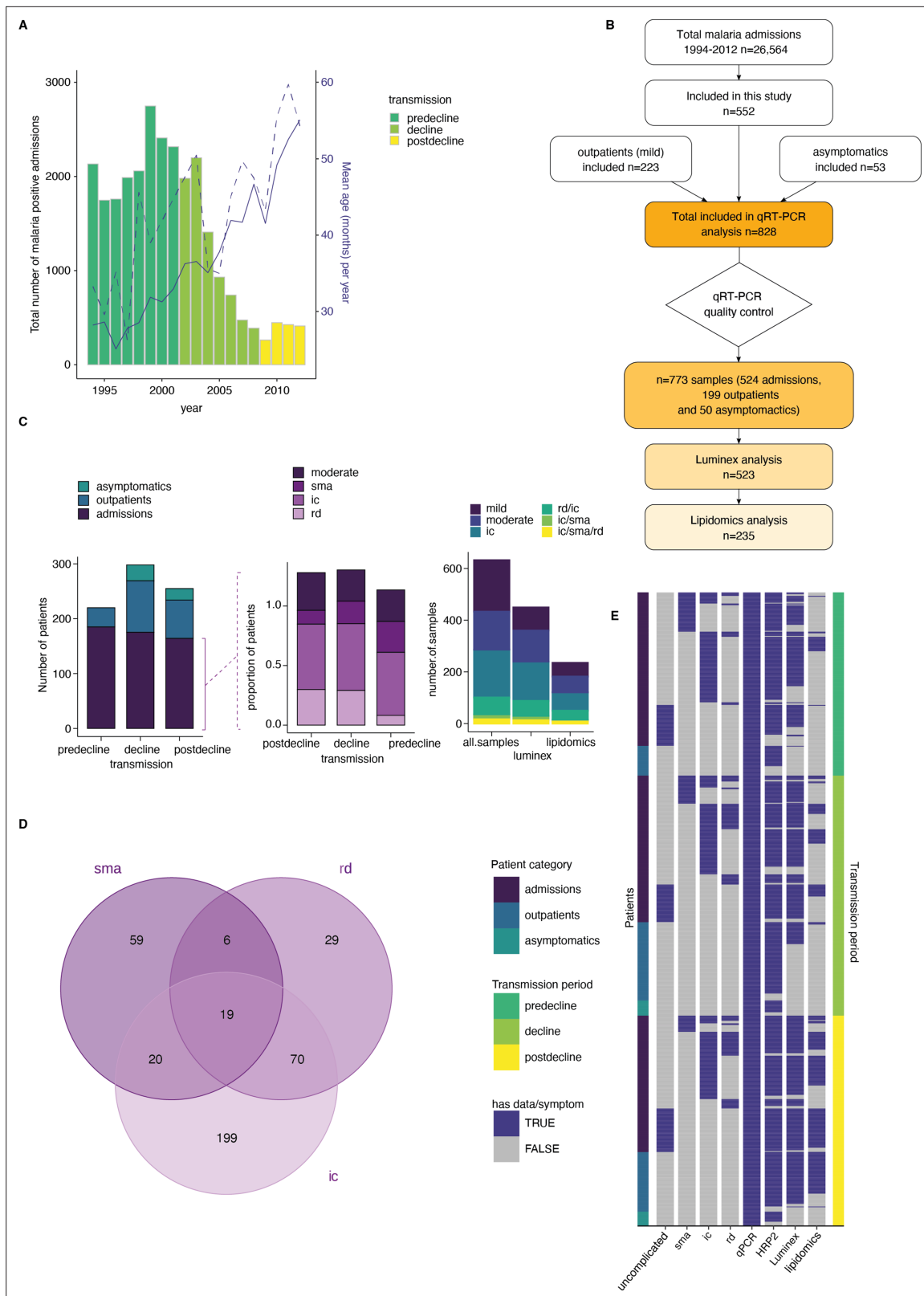
Figure 1. A clinical malaria patient cohort during changing the transmission in Kilifi, Kenya. (**A**) Total malaria admissions and patient age of the parent cohort. Number of patients per year (gray histogram, left axis). The solid blue line is the average patient age in the parent cohort, the dashed line is the average patient age in this study (both right axis). (**B**) Schematic of sample selection for this study. (**C**) Clinical presentation of patients selected for this study. Left: all patients, middle: admissions only, right: subset selected for luminex and lipidomics analysis. sma = severe malarial anemia, ic = impaired

Figure 1 continued on next page

Figure 1 continued

consiousness, rd = respiratory distress. (**D**) Number of patients in this study with different clinical presentations (402 severe cases initially selected). (**E**) Overview of the data available for each patient of the study, after excluding samples with *Pfsir2a* and *ap2-g* transcript transcription units greater or equal to 32 as described in the methods. Each row is one patient, organized by patient category (left axis) and transmission period (right axis).

of parasite-positive admissions decreased, the mean patient age at admission increased over time (*Marsh and Snow, 1999*; *White, 2018*; *Njuguna et al., 2019*; *Figure 1A*). For our study, 552 of the admissions were pragmatically selected to ensure adequate sampling of the transmission periods and clinical phenotypes (*Figure 1C*). 150 patients presented with moderate malaria and 402 with one or a combination of the severe malaria syndromes: impaired consciousness (IC), respiratory distress (RD), and severe malaria anemia (SMA) (*Marsh et al., 1995*; *Figure 1D*). 223 samples from children presenting with mild malaria at outpatient clinics and 53 asymptomatic children from a longitudinal malaria cohort study were added to cover the full range of the possible outcomes of malaria infection (*Figure 1B–E*), bringing the total number included in this study to 828 children. The characteristics of participants and clinical parameters are summarized in *Supplementary file 1*.

Dynamics of parasite parameters across transmission period and clinical phenotype

First, we analyzed the dynamics of parasite parameters across transmission periods and clinical outcomes. For this purpose, we measured both total parasite biomass based on *Pf*HRP2 levels (*Dondorp et al., 2005*) and peripheral parasitemia based on parasite counts from blood smears. Total parasite biomass (*Pf*HRP2) but not peripheral parasitemia decreased with declining transmission (*Figure 2A*). This decrease was significant in the patients presenting with mild malaria at outpatient clinics which is a more homogenous clinical subgroup as compared to admissions consisting of a range of clinical phenotypes (*Figure 1C–D*).

Parasite samples were subjected to qRT-PCR analysis to quantify transcription of *ap2-g*, *Pfsir2a*, and *var* gene subgroups relative to two housekeeping genes (fructose biphosphate aldolase and seryl tRNA synthetase) (*Salanti et al., 2003*; *Rottmann et al., 2006*; *Lavstsen et al., 2012*; *Abdi et al., 2016*). In line with recent findings (*Rono et al., 2018*), *ap2-g* transcription increased significantly with declining malaria transmission (*Figure 2B*, **left**). In the subsequent analysis, only clinical cases were considered. Asymptomatic patients were excluded except for analysis of clinical phenotype since asymptomatic sampling was limited to the decline and post-decline periods (*Figure 1C*), and, therefore, data could not be corrected for transmission.

Further analysis demonstrated that *ap2-g* transcription is highly significantly correlated with transcription levels of the gametocyte marker *Pfs16* (*Figure 2C*). This association validates *ap2-g* as a proxy for both, stage conversion and gametocyte levels. *Pfsir2a* transcription followed the same trend across transmission periods (*Figure 2B*, **right**) and was positively associated with *ap2-g* transcription (*Figure 2D*). *Pfsir2a* and *ap2-g* transcription also showed a positive association with fever (*Figure 2E*), suggesting that both factors are sensitive to changes in the host inflammatory response. *Pfsir2a* but not *ap2-g* transcription also showed a significant negative association with *Pf*HRP2 (*Figure 2D*). Given this unexpected observation, we investigated the well-established associations between *Pfsir2a* transcription and *var* gene transcription patterns (*Merrick et al., 2012*; *Abdi et al., 2016*). *Pfsir2a* transcription showed a positive association with global upregulation of *var* gene transcription, particularly with subgroup B (*Figure 2F*). Likewise, transcription of group B *var* subgroup, *Pfsir2a*, and *ap2-g* transcription followed a similar pattern in relation to clinical phenotypes (*Figure 2—figure supplement 1*). To ensure that there is no systematic bias in the qRT-PCR data, we also tested the association of *Pfs16* expression against *var* gene subgroups. *Pfs16* expression showed a significant positive correlation with group B (here termed gpb1) and C (gpc2) *var* genes, while no correlation was observed with the rest of the *var* subgroups (*Figure 3—figure supplement 1A*). Altogether these data suggest co-regulation of *ap2-g* and *Pfsir2a* and a negative association between *Pfsir2a* and *Pf*HRP2, likely through host factors that are changing with the declining transmission.
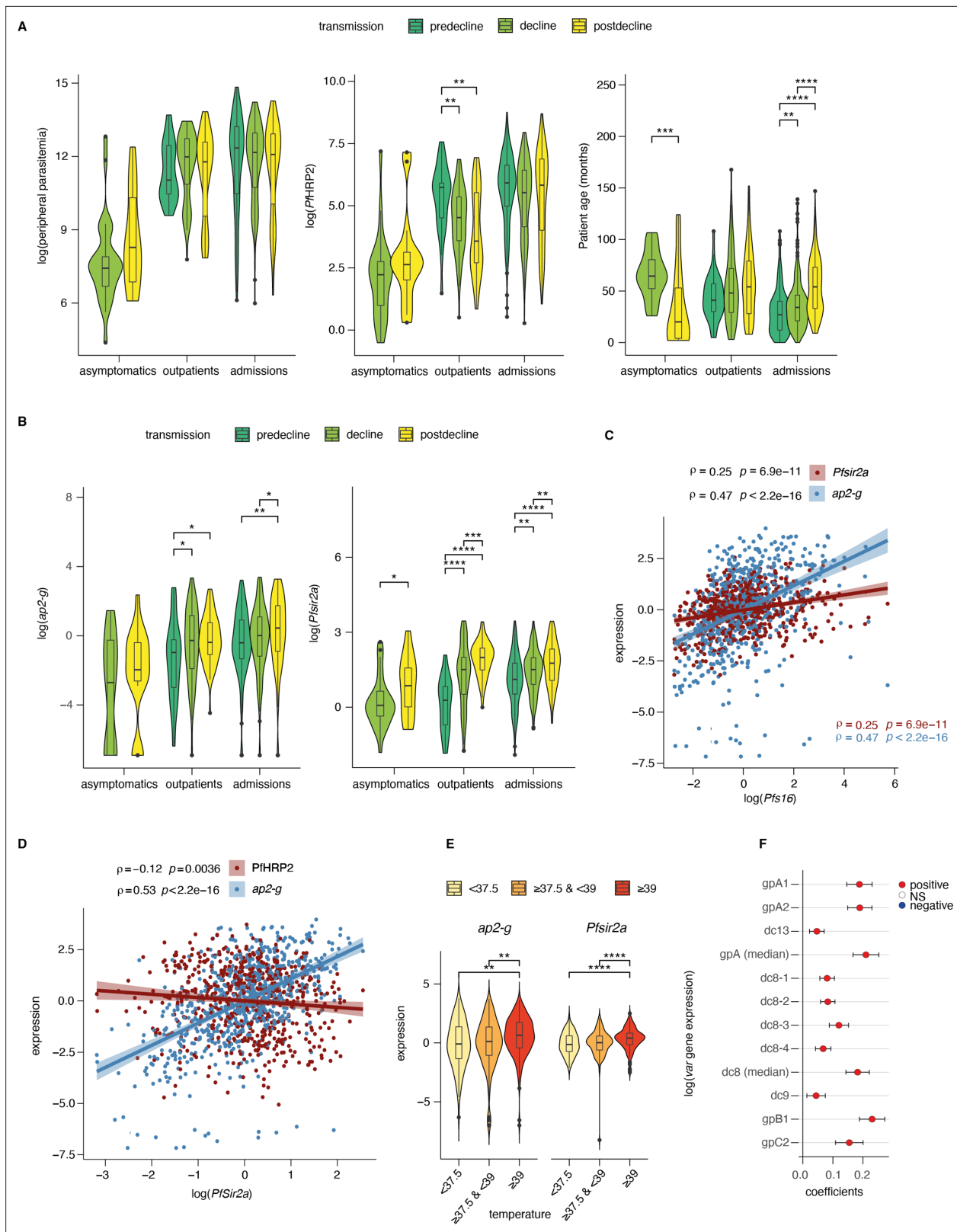
Figure 2. Dynamics of parasite parameters across transmission periods. (**A**) Peripheral parasitemia (smear, left), total parasite biomass (*Pf*HRP2, middle), and patient age (right) across patients. Number of patients: Asymptomatics: decline: n=29, postdecline: n=21; Outpatients: predecline: n=35, decline: n=94, postdecline: n=70; Admissions: predecline: n=185, decline: n=175, postdecline: n=164. (**B**) *ap2-g* transcript levels (left) and *Pfsir2a* levels (right) across patients. (**C**) Spearman's correlation between *Pfs16* and *ap2-g* (blue), or *PfSir2a* transcription (red) across patients (corrected for transmission). The

Figure 2 continued on next page

Figure 2 continued

lines fitted are linear regressions for visualization only. (**D**) Spearman's correlation between *Pfsir2a* and *ap2-g* transcription (blue), or *Pf*HRP2 levels (red) across patients (corrected for transmission). The lines fitted are linear regressions for visualization only. (**E**) *ap2-g* and *Pfsir2a* transcription (corrected for transmission) stratified by patient temperature. "<37.5": n=122, ">=37.5 & <39": n=228, ">=39": n=196. (**F**) Linear regression showing the association of *var* gene transcription levels with *Pfsir2a* levels (adjusted for transmission). 95% confidence intervals are shown. n=723 for all but c2 n=577. The color indicates whether the relationship is statistically significant (with Benjamini & Hochberg multiple tests correction). Positive correlations are in red, and negative in blue. gpA1, gpA2, and dc13 represent group A *var* gene transcripts. dc8-1 to dc8-4 represent DC8 *var* gene transcripts while gpb1 and gpc2 represent group B and C *var* genes. In the above graphs C-F (and all subsequent figures), asymptomatics were excluded in analyses involving the transmission period since they are not represented in the pre-decline period. All pairwise statistical tests indicated in the graphs are Wilcoxon tests corrected for multiple testing (Benjamini & Hochberg, *=FDR < 0.05, **=<0.01, ***=<0.001, and ****=<0.0001).

The online version of this article includes the following figure supplement(s) for figure 2:

Figure supplement 1. Parasite parameters stratified by clinical categories.

ap2-g and *Pfsir2a* transcription is associated with a distinct host inflammation profile

We hypothesized that the observed variation in *ap2-g* and *Pfsir2a* levels across the transmission period and clinical phenotype is due to underlying differences in the host inflammatory response. To test this hypothesis, we quantified 34 inflammatory markers (*Huang et al., 2017*) with Luminex xMAP technology in the plasma of the 523 patients from the outpatient and admissions groups (*Figure 1B*). These patients were selected from the original set of 828 to ensure adequate representation of the transmission periods and clinical phenotypes (including fever), as summarized in *Figure 1C and E*. For this analysis, all associations were corrected for patient age and *Pf*HRP2 levels as possible confounders.

The markers MCP-1, IL-10, IL-6, and IL-1ra were significantly positively correlated with *ap2-g* and *Pfsir2a* transcription (*Figure 3A* and *Figure 3—figure supplement 1B*). To cluster the inflammatory markers based on their correlation within the dataset, we used exploratory factor analysis and retained five factors with eigenvalues above 1 (*Figure 3—figure supplement 2*). Factor loadings structured the inflammation markers into five profiles with distinct inflammatory states (*Figure 3B*). F1 consists of a mixture of inflammatory markers that support effector Th1/Th2/Th9/Th17 responses (i.e. hyperinflammatory state), F2 represents a Th2 response, F3 represents markers that support follicular helper T cell development and Th17 (*Dong, 2021*; *Chao et al., 2023*), F4 represents markers of immune paralysis/tissue-injury linked to response to cellular/tissue injury (*Kumar et al., 2014*), and F5 represents the inflammasome/Th1 response (*Weiss et al., 2018*). F4 showed a significant positive association with *ap2-g* and *Pfsir2a* transcription and fever (*Figure 3C*). In contrast, F5 showed a negative association with *ap2-g* and fever while F1 was positively associated with fever (*Figure 3C*). In parallel with the observed decrease in *Pf*HRP2 levels (*Figure 2A*), F1 and F5 significantly declined with falling transmission (*Figure 3D*).

The data support our hypothesis and suggest that the host inflammatory response changes with the falling transmission. Of note, the observed negative association between *Pfsir2a* transcription and *Pf*HRP2 levels appears to be independent of the measured cytokine levels (*Figure 3—figure supplement 3*) and is hence likely the result of parasite intrinsic regulation of replication.

Plasma phospholipids link variation in the host inflammatory profile to *ap2-g* and *Pfsir2a* transcription

We have previously demonstrated in vitro that the serum phospholipid LPC serves as a substrate for parasite membrane biosynthesis during asexual replication, and as an environmental factor sensed by the parasite that triggers stage conversion (*Brancucci et al., 2017*). Plasma LPC is mainly derived from the turnover of phosphatidylcholine (PC) via phospholipase A2, while in the presence of Acyl-CoA the enzyme LPC acyltransferase (LPCAT) can drive the reaction in the other direction (*Law et al., 2019*; *Amunugama et al., 2021*). LPC is an inflammatory mediator that boosts type 1 immune response to eliminate pathogens (*Huang et al., 1999*; *Qin et al., 2014*). LPC turnover to PC can be triggered by inflammatory responses aimed to repair and restore tissue homeostasis rather than eliminate infection (*Law et al., 2019*). Here, we performed an unbiased lipidomics analysis of plasma from a representative subset of the outpatient and admission patients (*Figure 1* and *Figure 4—figure supplement 1*)
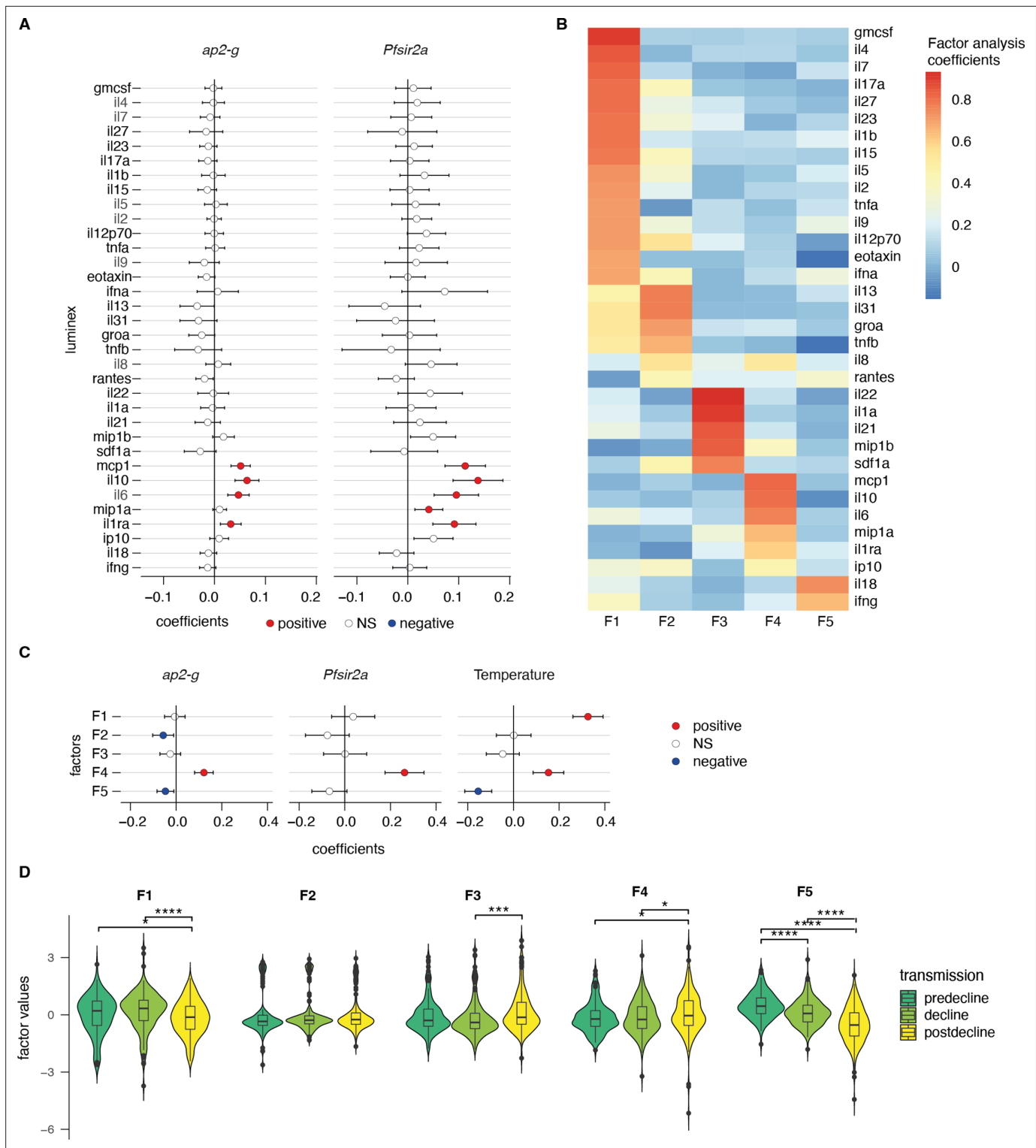
Figure 3. *ap2-g* and *Pfsir2a* transcription levels are associated with the host inflammation profile. (**A**) Association of inflammatory markers with *ap2-g* and *Pfsir2a* transcripts, tested using transmission period, age, and *Pf*HRP2 adjusted linear regression (*p*-values adjusted for multiple testing using Benjamini & Hochberg multiple tests correction). Plotted is the regression coefficient (estimate) and 95% CI. Above and below zero indicate statistically significant positive (red) and negative associations (blue), respectively. n=523 (**B**) Principal exploratory factor analysis. The figure shows the inflammatory marker loadings on the five factors (**F1–F5**) identified to have eigenvalue above 1. (**C**) Linear regression between inflammatory factors. (**F1–F5**) and *ap2-g* and *Pfsir2a* transcription and patient temperature (adjusted for transmission, *Pf*HRP2, and age). Plotted is the coefficient between the factor and the parameter (estimate) and 95% CI. Number of Patients: *ap2-g* and *Pfsir2a*: n=523, Temperature: n=496. The association is significant if the correlation

Figure 3 continued on next page

Figure 3 continued

FDR <0.05, in which case the positive associations are marked in red and the negative ones in blue. (**D**) Inflammatory factors stratified by transmission period. Pairwise tests are Wilcoxon tests (Benjamini & Hochberg, *=FDR < 0.05, **=<0.01, ***=<0.001, and ****=<0.0001). Number of patients: predecline: n=131, decline: n=180, postdecline: n=212.

The online version of this article includes the following figure supplement(s) for figure 3:

Figure supplement 1. Parasite and inflammatory markers stratified by transmission period.

Figure supplement 2. Factor loadings.

Figure supplement 3. Correcting *Plasmodium falciparum* histidine-rich protein 2 (*Pf*HRP2) vs *Pfsir2a* associations for external factors.

to explore whether the host inflammatory profile modifies the plasma lipid profile and consequently *ap2-g* and *Pfsir2a* transcription levels in vivo.

We examined associations between the host inflammatory factors (F1-F5) and the plasma lipidome data. Again, these associations were corrected for transmission period, patient age, and *Pf*HRP2 levels. 24 lipid species dominated by phospholipids, showed significant association with the inflammatory factors at a false discovery rate below 0.05 (*Figure 4A*). Like the observed associations with *ap2-g* and *Pfsir2a* transcription, cytokines in the F4 and F5 factors showed reciprocal associations with various LPC species and PC (*Figure 4A*): F5 showed a significant positive association with one LPC species and negative associations with PC, respectively, while F4 showed a significant negative association with three LPC species (*Figure 4A*, *Supplementary file 2*). The positive association of LPC with the F5 inflammatory factor is consistent with previous findings that identified LPC as an immunomodulator that can enhance IFN-γ production and the activation of the inflammasome (*Huang et al., 1999*; *Qin et al., 2014*), which results in increased levels of cytokines such as IL-18 (*Weiss et al., 2018*) and is necessary for eliminating parasites. Depletion of LPC is also associated with elevated markers of tissue injury (F4), perhaps following uncontrolled parasite growth or maladaptive inflammation. In summary, the association of inflammatory factors with lipids identified LPC, PC, and PE species as the most significant ones (*Figure 4A*), in line with their known immunomodulatory role. Importantly, we observed the same pattern in a controlled human infection model where parasite densities were allowed to rise to microscopic levels, both after sporozoite, and blood-stage infection (*Figure 4B* and *Figure 4—figure supplement 2*; *Alkema et al., 2021*; *Alkema et al., 2022*). Next, we examined the main lipid species associated with the five inflammatory factors with respect to *ap2-g* and *Pfsir2a* transcription. Indeed, LPC species showed a negative association with both *ap2-g* and *Pfsir2a* transcription levels (*Figure 4C–F*). The association was only significant in our data when inflammation is highest (and LPC level lowest), which is at low transmission (i.e. post decline). In contrast, LPC levels are highest and vary little across patients at high transmission (pre-decline).

Altogether, these data provide in vivo evidence for the previously observed link between LPC depletion and *ap2-g* activation and strongly suggest that LPC is both, a key immune modulator and a metabolite whose level is sensed by the parasite. Importantly, the key relationships described in *Figures 2–4* were independently significant in a structural equation model that examined how host immunity modifies the host-parasite interaction, the within-host environment, and parasite investment in transmission or replication (*Supplementary file 3*).

Discussion

Malaria parasites must adapt to changing environmental conditions across the life cycle in the mammalian and mosquito hosts. Similarly, changing conditions across seasons and transmission settings require both within- and between-host adaptation to optimize survival in the human host *versus* transmission to the next host. First, a recent transcriptomic study from Kenya and Sudan suggested that parasites in low transmission settings (where within-host competition is low) invest more in gametocyte production compared to high transmission settings (where within-host competition is high) (*Rono et al., 2018*). Second, a longitudinal study from Senegal demonstrated that human-to-mosquito transmission efficiency (and gametocyte density) increases when parasite prevalence in the human population decreases, suggesting that parasites can adapt to changes in the environment (*Churcher et al.,*
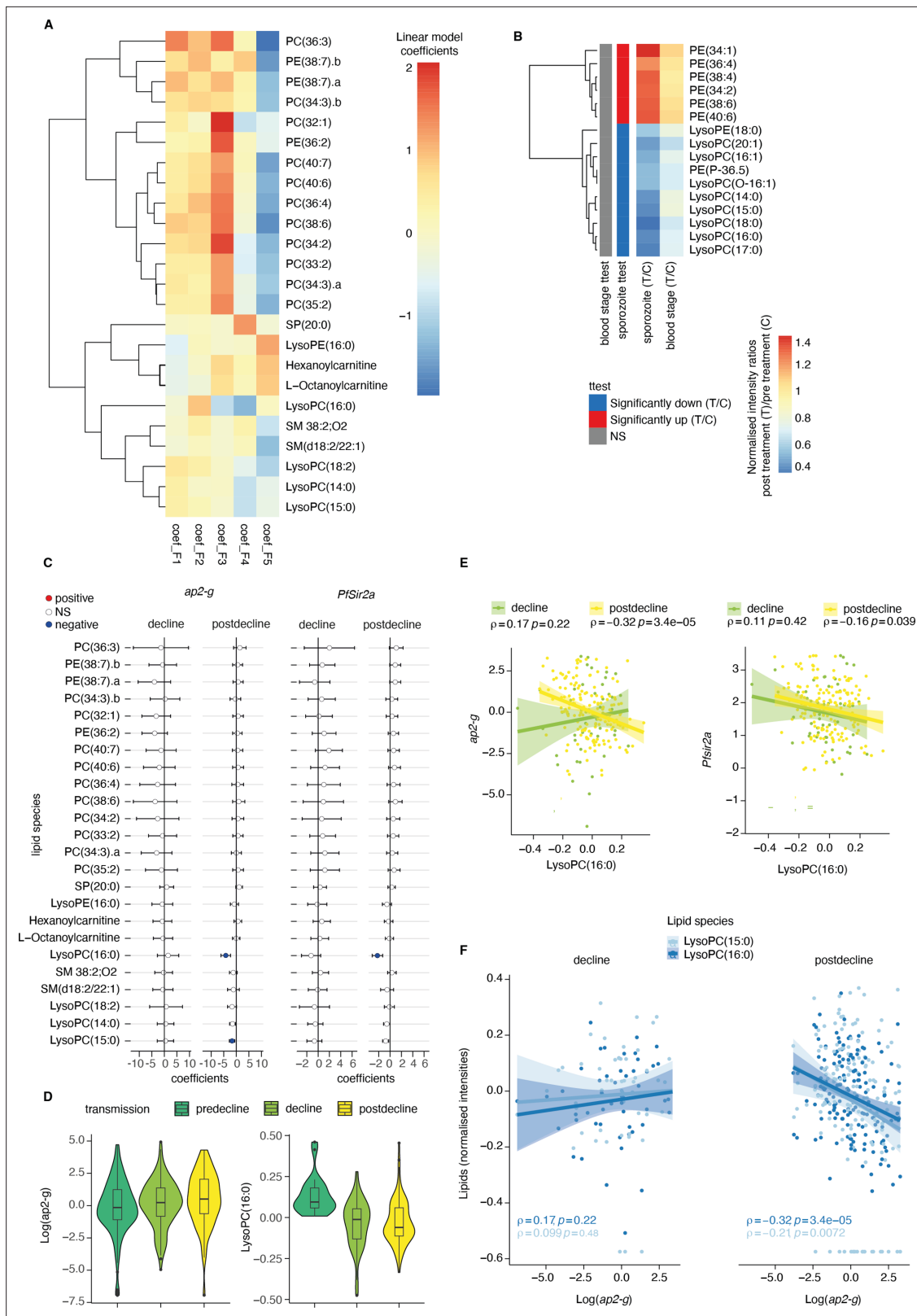
Figure 4. Plasma Lysophosphatidylcholine (LPC) links host inflammation to *ap2-g* and *Pfsir2a* transcription. (**A**) Heatmap of the linear regression coefficients between lipids and inflammatory factors (F1-F5, adjusted for transmission period and corrected for multiple testing). Shown are all lipids that are significantly associated (positive or negative) with factors F1-F5, clustered using R hclust (distance = Euclidean, method = centroid) and that have been manually identified and filtered for peak quality (isotopes and fragments weres also filtered out). (**B**) Shown are the lipids with significant

Figure 4 continued on next page

Figure 4 continued

differences (student's t-test corrected for multiple testing) between pre- and post-treatment in the controlled human malaria infections (CHMI) for either infection route (blood or sporozoite infection). Plotted is the fold-change post-treatment vs pre-treatment. On the left is indicated whether the lipid is significantly increased (red) or decreased (blue) in either route of infection. (**C**) Linear regression between the lipids from A and *ap2-g* or *Pfsir2a* transcription levels. Plotted is the coefficient and 95% CI. Blue indicates statistically significant negative correlations, while red indicates statically significant positive correlations (FDR <0.05). (**D**) Distribution of *ap2-g* transcript levels (left) and LysoPC (16:0) intensity (right) across patients and stratified by transmission period. Data are corrected for age and *Pf*HRP2. (**E**) Correlation between LPC (16:0) (top) and *ap2-g* (top), or *Pfsir2a* (bottom) transcription (Spearman's correlations corrected for multiple testing). (**F**) Correlations between identified LPCs and *ap2-g* transcription by transmission period (Spearman's correlations corrected for multiple testing). Note that the predecline period is not plotted separately in panels C-E due to insufficient sample numbers for the statistical analysis. Number of patients: predecline: n=22, decline: n=53, postdecline: n=160.

The online version of this article includes the following figure supplement(s) for figure 4:

Figure supplement 1. Sample subsetting and batch correction for lipidomics data.

Figure supplement 2. Controlled human malaria infections (CHMI) data.

2015). However, the within-host mechanisms driving parasite adaptation to the prevailing environment remain unclear.

Here, we analyzed parasite and host signatures in the plasma from a large malaria patient cohort over 18 years of declining malaria transmission in Kenya. This investigation allowed us to define some of the within-host environmental factors that change with transmission intensity and consequently influence the parasite's decision to invest in reproduction *versus* replication. A major strength of our study is that observations are from a single site and are thus plausibly reflective of transmission-related changes in parasite investments, rather than differences between geographically distinct parasite populations. We show that high transmission is associated with a host immune response that promotes parasite killing without compromising the intrinsic replicative ability of the individual parasite. In contrast, low transmission is associated with a host immune response that increases within-host stressors (fever, nutrient depletion), which trigger higher parasite investment into transmission (see also the model in *Figure 5*). Importantly, the observed associations between the parasite parameters *ap2-g*, *Pfsir2a,* and host inflammation remain significant if corrected for transmission, but they are strongest at low transmission (i.e. post decline period) when inflammation and the risk of damaging the host are highest. We anticipate that the proposed model could be tested in controlled human
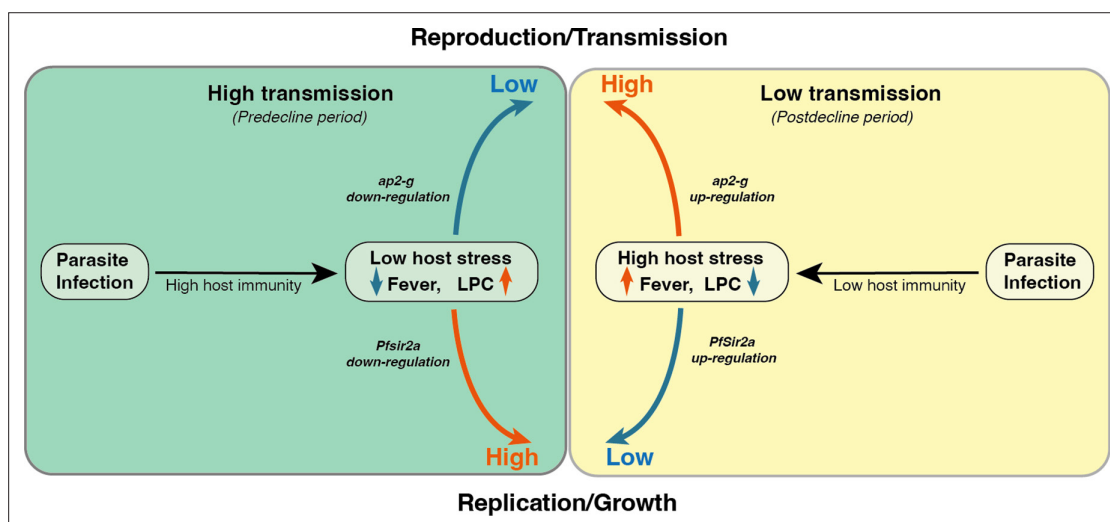
Figure 5. Proposed model on a within-host adaptation of the parasite to changing environments. The model is based on the interaction between the different host and parasite parameters described in this study. It proposes that declining transmission reduces host immunity, resulting in an inflammatory response associated with increased host stressors (including reduced Lysophosphatidylcholine (LPC) availability, and fever) and susceptibility to clinical symptoms/damage. The altered host response modifies the parasite response during infection, resulting in increased investment in transmission (as indicated by the elevated *ap2-g* levels) and reduced replication (as indicated by elevated *Pfsir2a* levels and reduced parasite burden/*Plasmodium falciparum* histidine-rich protein 2 (*Pf*HRP2) levels).

malaria infections with malaria naïve and semi-immune participants as a proxy for low vs high transmission settings.

At a systemic level, inflammation can influence the within-host environment and modulate parasite investment in replication *versus* reproduction by altering the levels of environmental stressors (e.g. oxidative, thermal, or nutritional stress). Consistent with this hypothesis, we show that a pro-inflammatory response mediated by IFN-γ/IL-18 (F5 in our analysis) promoting pathogen killing (*Weiss et al., 2018*; *Hoffman et al., 1997*; *Kearney et al., 2013*) is negatively associated with *ap2-g* and *Pfsir2a* transcription. In contrast, inflammatory markers that increase within-host environmental stress (e.g. fever) or reflect the extent of host tissue injury and are secreted to heal and restore homeostasis rather than kill pathogens (F4) (*Shapouri-Moghaddam et al., 2018*; *Tan et al., 2021*) are positively associated with *ap2-g* and *Pfsir2a* transcription. At a metabolic level, we previously demonstrated that LPC depletion induces *ap2-g* transcription and, therefore, gametocyte production in vitro (*Brancucci et al., 2017*). A recent study has provided the first indications of a possible association between LPC and *ap2-g* levels in a small malaria patient cohort (*Usui et al., 2019*). Here, we reveal that LPC levels are negatively associated with *ap2-g* transcription in patient plasma, thus providing direct evidence for our in vitro findings (*Brancucci et al., 2017*) across a large malaria patient cohort. LPC is an immune effector molecule promoting macrophage polarization to M1 phenotype that induces the secretion of various cytokines such as IFN-γ and IL-1 family (i.e. IL-18) (*Huang et al., 1999*; *Qin et al., 2014*) through activation of the inflammasome in endothelial cells and peripheral blood mononuclear cells (PBMCs). Furthermore, LPC is the main component of the oxidized form of LDL (oxLDL) that induces inflammasome-mediated trained immunity in human monocytes (*Law et al., 2019*; *Amunugama et al., 2021*), resulting in increased responsiveness to LPS re-stimulation. Indeed, we demonstrate that LPC levels are positively associated with IFN-γ/IL-18 levels (Factor 5). These observations are in line with recent data from experimentally infected macaques and malaria patients, where LPC levels decreased in the acute phase compared to the pre-challenge and the chronic phase (*Cordy et al., 2019*). LPC is also a nutritional resource required by the parasite for replication (*Brancucci et al., 2017*) and hence scarcity is expected to promote reproduction, as gametocytes require less nutritional resource and, therefore, provide a better adaptation strategy.

Surprisingly, we also identified a link between *Pfsir2a* transcription, host inflammatory response, and parasite biomass (*Pf*HRP2). *Pf*Sir2a belongs to the evolutionarily conserved family of sirtuins that act as environmental sensors to regulate various cellular processes (*Li, 2013*; *Vasquez et al., 2017*; *Palacios et al., 2009*). In *P. falciparum*, PfSir2a and PfSir2b paralogues cooperate to regulate virulence gene transcription including *var* genes (*Tonkin et al., 2009*; *Duraisingh et al., 2005*). In vitro data have also demonstrated that increased PfSir2a levels are associated with reduced parasite replication (i.e. lower merozoite numbers) (*Mancio-Silva et al., 2013*). We hypothesize that the observed upregulation of *Pfsir2a* transcription in response to inflammation is part of an orchestrated stress response linking replication and antigenic variation (via *Pfsir2a*) to reproduction and transmission (via *ap2-g*), perhaps through a shared epigenetic control mechanism (*Coleman et al., 2014*). It is well known that host tolerance to malaria infection reduces with falling transmission (*Borrmann et al., 2011*; *Dollat et al., 2019*), as shown by the declining threshold of parasite biomass (*Pf*HRP2) required for clinical malaria. This suggests that parasites have more pronounced harmful consequences on the infected host (i.e. clinical symptoms) in low compared to high transmission settings, perhaps due to increasing host age (*Sorci et al., 2021*). Under this scenario, we propose that parasites experience increased within-host stress to which they respond through increased *ap2-g* transcription (to increase reproduction, hence transmission) and increased *Pfsir2a* transcription (to affect stress coping mechanisms at the expense of replication, hence the negative association with *Pf*HRP2) – as part of a self-preservation strategy in the face of imminent risk of host death.

In summary, we propose a model where the falling host immunity with declining transmission modifies the predominant host immune response, and consequently, the within-host environment (e.g. LPC availability, fever), resulting in increased investment in transmission (i.e. higher *ap2-g* transcription) and limiting replication (i.e. higher *Pfsir2a* transcription). Our findings provide critical information to accurately model parasite population dynamics. They suggest that parasite populations in elimination scenarios may increase their transmission potential. Understanding how malaria parasites adapt to their environment, for example by increasing investment in transmission stages at low endemicity, is highly relevant for public health. Not only would this affect the timelines for successful elimination,

but it would also form an important argument for the deployment of gametocytocidal drugs once transmission has been successfully reduced.

Materials and methods

Study design and participants

Ethical approval was granted by the Scientific Ethics Review Unit of the Kenya Medical Research Institute under the protocol; KEMRI/SERU/3149, and informed consent was obtained from the parents/guardian of the children. The study was conducted in Kilifi county which is a malaria-endemic region along the Kenyan coast. Over the last three decades, Kilifi has experienced changes in the pattern of malaria transmission and clinical presentation spectrum (*O'Meara et al., 2008*; *Mogeni et al., 2016*; *Njuguna et al., 2019*). The study included (i) children admitted with malaria at Kilifi county hospital (KCH) between 1994–2012 and recruited as part of the hospital admission surveillance system, (ii) children presenting with mild malaria at an outpatient clinic, and (iii) asymptomatic children which were part of a longitudinal malaria surveillance cohort which were sampled during annual cross-section bleed in 2007 and 2010. Clinical data, parasite isolates, and plasma samples collected from the children were used to conduct the study. The selection of sub-samples for quantifying inflammatory markers and lipids was informed by the availability of fever data and resources.

Clinical definitions

Admission to malaria was defined as all hospitalized children with malaria parasitemia. The severe malaria syndromes: severe malarial anemia (SMA), impaired consciousness (IC), and respiratory distress (RD) were defined as hemoglobin <5 g/dl, Blantyre coma score (BCS) <5, and deep breathing, respectively (*Marsh et al., 1995*). Malaria admissions that did not present with either of the severe malaria syndromes were defined as moderate malaria. Mild malaria was defined as stable children presenting at the outpatient clinic with peripheral parasitemia, and asymptomatic as those with positive malaria (Giemsa smear) but without fever or any other sign(s) of illness. The combination of mild and moderate was referred to as uncomplicated.

Controlled infection cohort

Malaria naïve volunteers were infected by either bite from five *P. falciparum* 3D7–infected mosquitoes (n=12) or by intravenous injection with approximately 2800 *P. falciparum* 3D7–infected erythrocytes (n=12); treatment with piperaquine was provided at a parasite density of 5000 /mL or on day eight following blood-stage exposure, respectively (*Alkema et al., 2022*).

Parasite parameters

Thick and thin blood films were stained with Giemsa and examined for *P. falciparum* parasites according to standard methods. Data were presented as the number of infected RBCs per 500, 200, or 100 RBCs counted. This data was then used to calculate parasitemia per µl of blood using the formula described in '2096-OMS-GMP-SOP-09–20160222_v2.indd (who.int).' Briefly, parasites/µl=number of parasitized RBCs × number of RBCs per µl /number of RBCs counted or the number of parasites counted × number of WBCs per µl/number of WBCs counted. Where data on the actual number of RBCs or number of WBCs per µl of blood was not available, 5 million RBCs and 8000 WBCs per µl of blood were assumed.

PfHRP2 ELISA

P. falciparum histidine-rich protein 2 (*Pf*HRP2) was quantified in the malaria acute plasma samples using ELISA as outlined. Nunc MaxiSorp flat-bottom 96-well plates (ThermoFisher Scientific) were coated with 100 µl/well of the primary/capture antibody [Mouse anti-*Pf*HRP2 monoclonal antibody (MPFM-55A; MyBioscience)] in 1 × phosphate buffered saline (PBS) at a titrated final concentration of 0.9 µg/ml (stock = 8.53 mg/ml; dilution = 1:10,000) and incubated overnight at 4 °C. On the following day, the plates were washed thrice with 1 × PBS/0.05% Tween-20 (Sigma-Aldrich) using a BioTek ELx405 Select washer (BioTek Instruments, USA) and blotted on absorbent paper to remove residual buffer. These plates were then blocked with 200 µl/well of 1 × PBS/3% Marvel skimmed milk (Premier Foods; Thame, Oxford) and incubated for 2 hr at room temperature (RT) on a shaker

at 500 rpm. The plates were then washed thrice as before. After the final wash, plasma samples and standards were then added at 100 ul/well and in duplicates. The samples and standards (*Pf*HRP2 Recombinant protein; MBS232321, MyBioscience) had been appropriately diluted in 1 × PBS/2% bovine serum albumin (BSA). The samples and standards were incubated for 2 hr at RT on a shaker at 500 rpm followed by three washes with 1 × PBS/0.05% Tween-20 and blotted dry as before. This was followed by the addition of a 100 µl/well of the secondary/detection antibody [Mouse anti-*Pf*HRP2 HRP-conjugated antibody (MPFG-55P; MyBioscience) diluted in 1 × PBS/2% BSA and at a final titrated concentration of 0.2 µg/ml (stock = 1 mg/ml; dilution = 1:5000)]. The plates were then incubated for 1 hr at RT on a shaker at 500 rpm, washed thrice as before, and dried on absorbent paper towels. o-Phenylenediamine dihydrochloride (OPD) (ThermoFisher Scientific) substrate was then added at 100 µl/well and incubated for 15 min for color development. The reaction was stopped with 50 µl/well of 2 M sulphuric acid (H_2SO_4) and optical densities (OD) read at 490 nm with a BioTek Synergy4 reader (BioTek Instruments, USA).

Parasite transcript quantification using quantitative RT-PCR

RNA was obtained from TRIzol reagent (Invitrogen, catalog number 15596026) preserved *P. falciparum* positive venous blood samples obtained from the children recruited in the study. RNA was extracted by Chloroform method (*Bull et al., 2005*) and cDNA was synthesized using a Superscript III kit (Invitrogen, catalog number 18091050) following the manufacturer's protocol. Parasite gene transcription analysis was carried out through quantitative real-time PCR as described below.

Real-time PCR data was obtained as described (*Dondorp et al., 2005*; *Borrmann et al., 2011*; *Dollat et al., 2019*). Four primer pairs targeting DC8 (named dc8-1, dc8-2, dc8-3, dc8-4), one primer pair targeting DC13 (dc13), and two primer pairs targeting the majority of group A *var* genes (gpA1 and gpA2) were used in real-time PCR analysis as described (*Abdi et al., 2016*). We also used two primer pairs, b1, and c2, targeting group B and C *var* genes, respectively (*Rottmann et al., 2006*). Primer pairs targeting *Pfsir2a,* and *ap2-g* were also used (*Abdi et al., 2016*). Two housekeeping genes, Seryl tRNA synthetase and Fructose bisphosphate aldolase (*Salanti et al., 2003*; *Lavstsen et al., 2012*; *Abdi et al., 2016*) were used for relative quantification of the expressed *var* genes, *Pfsir2a,* and *ap2-g*. The PCR reaction and cycling conditions were carried out as described (*Lavstsen et al., 2012*; *Abdi et al., 2016*) using the Applied Biosystems 7500 Real-time PCR system. We set the cycle threshold (Ct) at 0.025. Controls with no template were included at the end of each batch of 22 samples per primer pair and the melt curves were analyzed for non-specific amplification. The *var* gene 'transcript quantity' was determined relative to the mean transcript of the two housekeeping genes, Sery tRNA synthetase and Fructose biphosphate aldolase as described (*Lavstsen et al., 2012*). For each test primer, the ΔCt was calculated relative to the average Ct of the two housekeeping genes which were then transformed to arbitrary transcript unit (Tu$_s$) using the formula (Tu$_s$ = $2^{(5-\Delta ct)}$) as described (*Lavstsen et al., 2012*). We assigned a zero Tu$_s$ value if a reaction did not result in detectable amplification after 40 cycles of amplification, that is, if the Ct value was undetermined.

Measurement of cytokine levels in the plasma samples

The selection for this subset was primarily informed by the availability of fever data but the transmission period and clinical phenotype were also considered. However, there were more children with a fever data recorded in the post-decline period than in pre-decline and decline periods which biased the sampling toward the post-decline period. The plasma samples were analyzed using Procarta-Plex Human Cytokine & Chemokine Panel 1 A(34plex) [Invitrogen/ThermoFisher Scientific; catalog # EPX340-12167-901; Lot:188561049] following the manufacturer's instructions. The following 34 cytokines were measured: GM-CSF, IFN-α, IFN-γ, IL-1α, IL-1β, IL-1RA, IL-2, IL-4, IL-5, IL-6, IL-7, IL-8, IL-9, IL-10, IL-12 (p70), IL-13, IL-15, IL-17A, IL-18, IL-21, IL-22, IL-23, IL-27, IL-31, IP-10 (CXCL10), MCP-1 (CCL2), MIP-1α (CCL3), MIP-1β (CCL4), TNF-α, TNF-β, Eotaxin/CCL11, RANTES, GRO-a, and SDF-1a.

Briefly, 50 µl of magnetic beads mix was added into each plate well and the 96-well plate was securely placed on a hand-held magnetic plate washer for 2 min for the beads to settle. The liquid was then removed by carefully inverting the plate over a waste container while still on the magnet and lightly blotted on absorbent paper towels. The beads were then washed by adding 150 µl of 1 × wash buffer, left to settle for 2 min, and the liquid removed as before followed by blotting. This was followed by adding 25 µl of Universal Assay Buffer per well and then 25 µl of plasma samples and standards into

appropriate wells or 25 µl of Universal Assay Buffer in blank wells. The plate was covered and shaken on a plate shaker at 500 rpm for 30 min at room temperature followed by an overnight incubation at 4 °C. After the overnight incubation, the plate was shaken on a plate shaker at 500 rpm for 30 min at room temperature and the beads were then washed twice while on a magnetic plate holder as outlined above. The beads were then incubated in the dark with 25 µl of detection antibody mixture on a plate shaker at 500 rpm for 30 min at room temperature followed by two washes as before. A 50 µl of Streptavidin-Phycoerythrin (SAPE) solution was then added per well and similarly incubated for 30 min on a plate shaker at 500 rpm and at room temperature followed by two washes. After the final wash, the beads were resuspended in 120 µl of Reading Buffer per well, and incubated for 5 min on a plate shaker at 500 rpm before running on a MAGPIX reader running on MAGPIX xPOTENT 4.2 software (Luminex Corporation). The instrument was set to count 100 beads for each analyte. The analyte concentrations were calculated (via Milliplex Analyst v5.1 [VigeneTech]) from the median fluorescence intensity (MdFI) expressed in pg/mL using the standard curves of each cytokine.

Lipidomics analysis

Patient temperature, *ap2-g* transcription level, and disease type were used to subset samples for lipidomics. This resulted in five groups from severe disease categories and matching mild cases (*Figure 4—figure supplement 1*). Plasma samples were preserved at –80 °C until extraction with the chloroform/methanol method. 25 µL of plasma was extracted with 1 mL of the extraction solvent chloroform/methanol/water (1:3:1 ratio), the tubes were rocked for 10 min at 4 °C and centrifuged for 3 min at 13,000 g. Supernatant was collected and stored at –80 °C in glass tubes until analysis.

Sample vials were placed in the autosampler tray in random order and kept at 5 °C. Separation was performed using a Dionex UltiMate 3000 RSLC system (Thermo Scientific, Hemel Hempstead) by injection of 10 µl sample onto a silica gel column (150 mm × 3 mm × 3 µm; HiChrom, Reading, UK) used in hydrophilic interaction chromatography (HILIC) mode held at 30°C (*Zheng et al., 2010*). Two solvents were used: solvent A [20% isopropyl alcohol (IPA) in acetonitrile] and solvent B [20% IPA in ammonium formate (20 mM)]. Elution was achieved using the following gradient at 0.3 ml/min: 0–1 min 8% B, 5 min 9% B, 10 min 20% B, 16 min 25% B, 23 min 35% B, and 26–40 min 8% B. Detection of lipids were performed in a Thermo Orbitrap Fusion mass spectrometer (Thermo Fisher Scientific Inc, Hemel Hempstead, UK) in polarity switching mode. The instrument was calibrated according to the manufacturer's specifications to give an rms mass error <1 ppm. The following electrospray ionization settings were used: source voltage, ±4.30 kV; capillary temp, 325 °C; sheath gas flow, 40 arbitrary units (AU); auxiliary gas flow, 5 AU; sweep gas flow, 1 AU. All LC-MS spectra were recorded in the range of 100–1200 at 120,000 resolutions (FWHM at m/z 500).

Data preprocessing

The raw data were converted to mzML files using proteowizard (v 3.0.9706 (2016-5-12)). These files were then analyzed using R (v 4.2.1) libraries xcms (v 3.14.1) and mzmatch 2 (v 1.0–4) for peak picking, alignment, filtering, and annotations (*Chong and Xia, 2018*; *Scheltema et al., 2011*; *Smith et al., 2006*). Batch correction was applied as in (https://www.mdpi.com/2218-1989/10/6/241/htm), and the data was then checked using PCA calculated using the R function prcomp (see *Figure 4—figure supplement 1*). Data was then range normalized and logged transformed using MetaboanalystR (v3.1.0). The CHMI lipidomics data was analyzed the same way but did not require batch correction as the samples were run in one batch.

Statistical analysis

Data analysis was performed using R (v4.2.1) except for the structural equation modeling which was done in Mplus8. We normalized non-normally distributed variables by log transformation. *qRT-PCR:* Zeros in qRT-PCR values were replaced by 0.001 (the value before log transformation as the smallest measured value is about 0.0017). The median transcript units from qRT-PCR were calculated as follows: DC8 median from four primer pairs used (DC8-1, DC8-2, DC8-3, and DC8-4) and group A median from three primer pairs (gpA1, gpA2, and dc13). Samples for which *ap2-g* or *pfsir2a* arbitrary transcript unit was greater or equal to 32 (that is the transcript quantity of the reference genes based on the formula ($Tu_s = 2^{(5-\Delta ct)}$) *Zheng et al., 2010*) were deemed unreliable and excluded from the analysis that went into generating *Figures 2–4*. Comparison between the two groups was done

using a two-sided Wilcoxon test. All correlations were conducted using Spearman's rank correlation coefficient test. All forest plots were done using linear regressions adjusted for transmission period, *Pf*HRP2, and age of the patient (see figure legends) using R function lm. All multiple test corrections were done using Benjamini & Hochberg multiple tests (using R function p.adjust).

Principal factor analysis

A measurement model (i.e. factor analytic model) was fitted to summarize the 34 analytes into fewer variables called factors. An exploratory factor analysis (EFA) was performed to explore the factor structure underlying the 34 analytes. Factors were retained based on the Kaiser's 'eigenvalue rule' of retaining eigenvalues larger than 1. In addition, we also considered the scree plot, parallel analysis, fit statistics, and interpretability of the model/factors. This analysis resulted in the cytokine data being reduced to five factors. This analysis was done using the R 'psych' library (v 2.1.9) available at https://CRAN.R-project.org/package=psych. The 34 analytes were individually linearly regressed to *ap2-g* or *Pfsir2* transcript levels with the transmission, *Pf*HRP2, and age correction (model: analyte ~transmission + *Pf*HRP2 +age). Then each factor was analyzed the same way.

Lipidomics analysis

The preprocessed lipidomics data was tested using transmission period, *Pf*HRP2, and age-adjusted linear regression with any of the five factors. All m/z with a significant false discovery rate with any of the factors were then manually checked for peak quality and identified masses on mass and retention time (*Reis et al., 2013*). The remaining identified lipids were then checked for the relationship with *ap2-g* and *Pfsir2a* transcription levels (linear regression adjusted for transmission period, HRP, and age, see methods above). The CHMI lipidomics data was analyzed the same way but the peaks retained were those significantly different pre and post-treatment in either type of infection (student's t-tests corrected for multiple testing).

Figures

All heatmaps were done using the R library pheatmap (v 1.0.12) available at https://CRAN.R-project.org/package=pheatmap, and all other plots using the R libraries ggplot2 (v 3.3.5) and ggpubr (v 0.4.0) available at https://CRAN.R-project.org/package=ggpubr.

Acknowledgements

Additional information

Author contributions

Author ORCIDs

Fiona Achcar http://orcid.org/0000-0001-8792-7615
João Luiz Silva-Filho http://orcid.org/0000-0003-4762-2205
Shaban Mwangi http://orcid.org/0000-0003-1961-3205
Manon Alkema http://orcid.org/0000-0002-8906-0047
Teun Bousema http://orcid.org/0000-0003-2666-094X
Matthias Marti http://orcid.org/0000-0003-1040-9566

Ethics

Ethical approval was granted by the Scientific Ethics Review Unit of the Kenya Medical Research Institute under the protocol; KEMRI/SERU/3149, and informed consent was obtained from the parents/guardian of the children.

Decision letter and Author response

Decision letter https://doi.org/10.7554/eLife.85140.sa1
Author response https://doi.org/10.7554/eLife.85140.sa2

Additional files

Supplementary files

- Supplementary file 1. Associations between parasite parameters *ap2-g*, *Pfsir2-a* and *Pf*HRP2, and clinical parameters.

- Supplementary file 2. Associations between parasite parameters *ap2-g*, *Pfsir2-a* and *Pf*HRP2, host luminex markers, and lipidomics data.

- Supplementary file 3. Structural equation model (SEM). The model assumes that pre-existing host immunity affects the interaction between the host (i.e. altered within the host environment including inflammatory response. fever, nutritional resource availability) and parasite (i.e. altered investment in reproduction *vs* replication). Significant *p*-values are highlighted in bold and negative and positive estimates of associations are highlighted in blue and red, respectively.

- MDAR checklist

Data availability

Raw data and script for all the analyses in this manuscript are available at https://doi.org/10.7910/DVN/BXXVRY. mzML mass spectrometry files are available at MetaboLights at https://www.ebi.ac.uk/metabolights/editor/study/MTBLS5130.

The following datasets were generated:

Author(s)	Year	Dataset title	Dataset URL	Database and Identifier
Abdi AI, Achcar F, Sollelis L, Silva-Filho JL, Mwikali K, Muthui M, Mwangi S, Kimingi HW, Orindi B, Kivisi CA, Alkema M, Chandrasekar A, Bull PC, Bejon P, Modrzynska K, Bousema T, Marti M	2023	*Plasmodium falciparum* adapts its investment into replicationversustransmission according to the host environment	https://www.ebi.ac.uk/metabolights/editor/study/MTBLS5130	EBI, MTBLS5130
Abdi AI, Achcar F, Sollelis L, Silva-Filho JL, Mwikali K, Muthui M, Mwangi S, Kimingi HW, Orindi B, Kivisi CA, Alkema M, Chandrasekar A, Bull PC, Bejon P, Modrzynska K, Bousema T, Marti M	2023	Replication Data for: Plasmodium falciparum adapts investment into replication versus reproduction transmission according to host environment	https://doi.org/10.7910/DVN/BXXVRY	Harvard Dataverse, 10.7910/DVN/BXXVRY

References

Abdi AI, Warimwe GM, Muthui MK, Kivisi CA, Kiragu EW, Fegan GW, Bull PC. 2016. Global selection of *Plasmodium falciparum* virulence antigen expression by host antibodies. *Scientific Reports* **6**:19882. DOI: https://doi.org/10.1038/srep19882, PMID: 26804201

Alkema M, Reuling IJ, de Jong GM, Lanke K, Coffeng LE, van Gemert GJ, van de Vegte-Bolmer M, de Mast Q, van Crevel R, Ivinson K, Ockenhouse CF, McCarthy JS, Sauerwein R, Collins KA, Bousema T. 2021. A randomized clinical trial to compare *Plasmodium falciparum* gametocytemia and infectivity after blood-stage or mosquito bite-induced controlled malaria infection. *The Journal of Infectious Diseases* **224**:1257–1265. DOI: https://doi.org/10.1093/infdis/jiaa157, PMID: 32239171

Alkema M, Yap XZ, de Jong GM, Reuling IJ, de Mast Q, van Crevel R, Ockenhouse CF, Collins KA, Bousema T, McCall MBB, Sauerwein RW. 2022. Controlled human malaria infections by mosquito bites induce more severe clinical symptoms than asexual blood-stage challenge infections. *EBioMedicine* **77**:103919. DOI: https://doi.org/10.1016/j.ebiom.2022.103919, PMID: 35278741

Amunugama K, Pike DP, Ford DA. 2021. The lipid biology of sepsis. *Journal of Lipid Research* **62**:100090. DOI: https://doi.org/10.1016/j.jlr.2021.100090, PMID: 34087197

Borrmann S, Sasi P, Mwai L, Bashraheil M, Abdallah A, Muriithi S, Frühauf H, Schaub B, Pfeil J, Peshu J, Hanpithakpong W, Rippert A, Juma E, Tsofa B, Mosobo M, Lowe B, Osier F, Fegan G, Lindegårdh N, Nzila A, et al. 2011. Declining responsiveness of *Plasmodium falciparum* infections to artemisinin-based combination treatments on the kenyan coast. *PLOS ONE* **6**:e26005. DOI: https://doi.org/10.1371/journal.pone.0026005, PMID: 22102856

Bosch-Presegué L, Vaquero A. 2014. Sirtuins in stress response: guardians of the genome. *Oncogene* **33**:3764–3775. DOI: https://doi.org/10.1038/onc.2013.344, PMID: 23995787

Brancucci NMB, Gerdt JP, Wang C, De Niz M, Philip N, Adapa SR, Zhang M, Hitz E, Niederwieser I, Boltryk SD, Laffitte MC, Clark MA, Grüring C, Ravel D, Blancke Soares A, Demas A, Bopp S, Rubio-Ruiz B, Conejo-Garcia A, Wirth DF, et al. 2017. Lysophosphatidylcholine regulates sexual stage differentiation in the human malaria parasite *Plasmodium falciparum*. *Cell* **171**:1532–1544. DOI: https://doi.org/10.1016/j.cell.2017.10.020, PMID: 29129376

Buckling A, Ranford-Cartwright LC, Miles A, Read AF. 1999. Chloroquine increases *Plasmodium falciparum* gametocytogenesis in vitro. *Parasitology* **118 (Pt 4)**:339–346. DOI: https://doi.org/10.1017/s0031182099003960, PMID: 10340323

Bull PC, Berriman M, Kyes S, Quail MA, Hall N, Kortok MM, Marsh K, Newbold CI. 2005. *Plasmodium falciparum* variant surface antigen expression patterns during malaria. *PLOS Pathogens* **1**:e26. DOI: https://doi.org/10.1371/journal.ppat.0010026, PMID: 16304608

Carter R, Miller LH. 1979. Evidence for environmental modulation of gametocytogenesis in *Plasmodium falciparum* in continuous culture. *Bulletin of the World Health Organization* **57 Suppl 1**:37–52 PMID: 397008.

Chao YY, Puhach A, Frieser D, Arunkumar M, Lehner L, Seeholzer T, Garcia-Lopez A, van der Wal M, Fibi-Smetana S, Dietschmann A, Sommermann T, Ćiković T, Taher L, Gresnigt MS, Vastert SJ, van Wijk F, Panagiotou G, Krappmann D, Groß O, Zielinski CE. 2023. Human th17 cells engage gasdermin E pores to release IL-1α on NLRP3 inflammasome activation. *Nature Immunology* **24**:295–308. DOI: https://doi.org/10.1038/s41590-022-01386-w, PMID: 36604548

Chong J, Xia J. 2018. MetaboAnalystR: an R package for flexible and reproducible analysis of metabolomics data. *Bioinformatics* **34**:4313–4314. DOI: https://doi.org/10.1093/bioinformatics/bty528, PMID: 29955821

Churcher TS, Trape JF, Cohuet A. 2015. Human-to-mosquito transmission efficiency increases as malaria is controlled. *Nature Communications* **6**:6054. DOI: https://doi.org/10.1038/ncomms7054, PMID: 25597498

Coleman BI, Skillman KM, Jiang RHY, Childs LM, Altenhofen LM, Ganter M, Leung Y, Goldowitz I, Kafsack BFC, Marti M, Llinás M, Buckee CO, Duraisingh MT. 2014. A *Plasmodium falciparum* histone deacetylase regulates antigenic variation and gametocyte conversion. *Cell Host & Microbe* **16**:177–186. DOI: https://doi.org/10.1016/j.chom.2014.06.014, PMID: 25121747

Cordy RJ, Patrapuvich R, Lili LN, Cabrera-Mora M, Chien JT, Tharp GK, Khadka M, Meyer EV, Lapp SA, Joyner CJ, Garcia A, Banton S, Tran V, Luvira V, Rungin S, Saeseu T, Rachaphaew N, Pakala SB, DeBarry JD, Kissinger JC, et al. 2019. Distinct amino acid and lipid perturbations characterize acute versus chronic malaria. *JCI Insight* **4**:e125156. DOI: https://doi.org/10.1172/jci.insight.125156, PMID: 31045574

Dollat M, Talla C, Sokhna C, Diene Sarr F, Trape JF, Richard V. 2019. Measuring malaria morbidity in an area of seasonal transmission: pyrogenic parasitemia thresholds based on a 20-year follow-up study. *PLOS ONE* **14**:e0217903. DOI: https://doi.org/10.1371/journal.pone.0217903, PMID: 31246965

Dondorp AM, Desakorn V, Pongtavornpinyo W, Sahassananda D, Silamut K, Chotivanich K, Newton PN, Pitisuttithum P, Smithyman AM, White NJ, Day NPJ. 2005. Estimation of the total parasite biomass in acute falciparum malaria from plasma pfhrp2. *PLOS Medicine* **2**:e204. DOI: https://doi.org/10.1371/journal.pmed.0020204, PMID: 16104831

Dong C. 2021. Cytokine regulation and function in T cells. *Annual Review of Immunology* **39**:51–76. DOI: https://doi.org/10.1146/annurev-immunol-061020-053702, PMID: 33428453

Duraisingh MT, Voss TS, Marty AJ, Duffy MF, Good RT, Thompson JK, Freitas-Junior LH, Scherf A, Crabb BS, Cowman AF. 2005. Heterochromatin silencing and locus repositioning linked to regulation of virulence genes in *Plasmodium falciparum. Cell* **121**:13–24. DOI: https://doi.org/10.1016/j.cell.2005.01.036, PMID: 15820675

Hanson J, Lam SWK, Mahanta KC, Pattnaik R, Alam S, Mohanty S, Hasan MU, Hossain A, Charunwatthana P, Chotivanich K, Maude RJ, Kingston H, Day NP, Mishra S, White NJ, Dondorp AM. 2012. Relative contributions of macrovascular and microvascular dysfunction to disease severity in falciparum malaria. *The Journal of Infectious Diseases* **206**:571–579. DOI: https://doi.org/10.1093/infdis/jis400, PMID: 22693227

Hoffman SL, Crutcher JM, Puri SK, Ansari AA, Villinger F, Franke ED, Singh PP, Finkelman F, Gately MK, Dutta GP, Sedegah M. 1997. Sterile protection of monkeys against malaria after administration of interleukin-12. *Nature Medicine* **3**:80–83. DOI: https://doi.org/10.1038/nm0197-80, PMID: 8986746

Huang YH, Schäfer-Elinder L, Wu R, Claesson HE, Frostegård J. 1999. Lysophosphatidylcholine (LPC) induces proinflammatory cytokines by a platelet-activating factor (PAF) receptor-dependent mechanism. *Clinical and Experimental Immunology* **116**:326–331. DOI: https://doi.org/10.1046/j.1365-2249.1999.00871.x, PMID: 10337026

Huang DTN, Lu CY, Chi YH, Li WL, Chang LY, Lai MJ, Chen JS, Hsu WM, Huang LM. 2017. Adaptation of influenza A (H7N9) virus in primary human airway epithelial cells. *Scientific Reports* **7**:11300. DOI: https://doi.org/10.1038/s41598-017-10749-5, PMID: 28900138

Kafsack BFC, Rovira-Graells N, Clark TG, Bancells C, Crowley VM, Campino SG, Williams AE, Drought LG, Kwiatkowski DP, Baker DA, Cortés A, Llinás M. 2014. A transcriptional switch underlies commitment to sexual development in malaria parasites. *Nature* **507**:248–252. DOI: https://doi.org/10.1038/nature12920, PMID: 24572369

Kearney S, Delgado C, Lenz LL. 2013. Differential effects of type I and II interferons on myeloid cells and resistance to intracellular bacterial infections. *Immunologic Research* **55**:187–200. DOI: https://doi.org/10.1007/s12026-012-8362-y, PMID: 22983898

Kumar M, Seeger W, Voswinckel R. 2014. Senescence-associated secretory phenotype and its possible role in chronic obstructive pulmonary disease. *American Journal of Respiratory Cell and Molecular Biology* **51**:323–333. DOI: https://doi.org/10.1165/rcmb.2013-0382PS, PMID: 25171460

Langhorne J, Ndungu FM, Sponaas AM, Marsh K. 2008. Immunity to malaria: more questions than answers. *Nature Immunology* **9**:725–732. DOI: https://doi.org/10.1038/ni.f.205, PMID: 18563083

Lavstsen T, Turner L, Saguti F, Magistrado P, Rask TS, Jespersen JS, Wang CW, Berger SS, Baraka V, Marquard AM, Seguin-Orlando A, Willerslev E, Gilbert MTP, Lusingu J, Theander TG. 2012. *Plasmodium falciparum* erythrocyte membrane protein 1 domain cassettes 8 and 13 are associated with severe malaria in children. *PNAS* **109**:E1791–E1800. DOI: https://doi.org/10.1073/pnas.1120455109, PMID: 22619319

Law SH, Chan ML, Marathe GK, Parveen F, Chen CH, Ke LY. 2019. An updated review of lysophosphatidylcholine metabolism in human diseases. *International Journal of Molecular Sciences* **20**:1149. DOI: https://doi.org/10.3390/ijms20051149, PMID: 30845751

Li X. 2013. Sirt1 and energy metabolism. *Acta Biochimica et Biophysica Sinica* **45**:51–60. DOI: https://doi.org/10.1093/abbs/gms108, PMID: 23257294

Mancio-Silva L, Lopez-Rubio JJ, Claes A, Scherf A. 2013. Sir2a regulates rdna transcription and multiplication rate in the human malaria parasite *Plasmodium falciparum. Nature Communications* **4**:1530. DOI: https://doi.org/10.1038/ncomms2539, PMID: 23443558

Marsh K, Forster D, Waruiru C, Mwangi I, Winstanley M, Marsh V, Newton C, Winstanley P, Warn P, Peshu N. 1995. Indicators of life-threatening malaria in african children. *The New England Journal of Medicine* **332**:1399–1404. DOI: https://doi.org/10.1056/NEJM199505253322102, PMID: 7723795

Marsh K, Snow RW. 1999. Malaria transmission and morbidity. *Parassitologia* **41**:241–246 PMID: 10697862.

Merrick CJ, Huttenhower C, Buckee C, Amambua-Ngwa A, Gomez-Escobar N, Walther M, Conway DJ, Duraisingh MT. 2012. Epigenetic dysregulation of virulence gene expression in severe *Plasmodium falciparum* malaria. *The Journal of Infectious Diseases* **205**:1593–1600. DOI: https://doi.org/10.1093/infdis/jis239, PMID: 22448008

Mogeni P, Williams TN, Fegan G, Nyundo C, Bauni E, Mwai K, Omedo I, Njuguna P, Newton CR, Osier F, Berkley JA, Hammitt LL, Lowe B, Mwambingu G, Awuondo K, Mturi N, Peshu N, Snow RW, Noor A, Marsh K, et al. 2016. Age, spatial, and temporal variations in hospital admissions with malaria in kilifi county, kenya: a 25-year longitudinal observational study. *PLOS Medicine* **13**:e1002047. DOI: https://doi.org/10.1371/journal.pmed.1002047, PMID: 27352303

Njuguna P, Maitland K, Nyaguara A, Mwanga D, Mogeni P, Mturi N, Mohammed S, Mwambingu G, Ngetsa C, Awuondo K, Lowe B, Adetifa I, Scott JAG, Williams TN, Atkinson S, Osier F, Snow RW, Marsh K, Tsofa B, Peshu N, et al. 2019. Observational study: 27 years of severe malaria surveillance in kilifi, kenya. *BMC Medicine* **17**:124. DOI: https://doi.org/10.1186/s12916-019-1359-9, PMID: 31280724

Oakley MSM, Kumar S, Anantharaman V, Zheng H, Mahajan B, Haynes JD, Moch JK, Fairhurst R, McCutchan TF, Aravind L. 2007. Molecular factors and biochemical pathways induced by febrile temperature in intraerythrocytic *Plasmodium falciparum* parasites. *Infection and Immunity* **75**:2012–2025. DOI: https://doi.org/10.1128/IAI.01236-06, PMID: 17283083

O'Meara WP, Bejon P, Mwangi TW, Okiro EA, Peshu N, Snow RW, Newton C, Marsh K. 2008. Effect of a fall in malaria transmission on morbidity and mortality in kilifi, kenya. *Lancet* **372**:1555–1562. DOI: https://doi.org/10.1016/S0140-6736(08)61655-4, PMID: 18984188

Palacios OM, Carmona JJ, Michan S, Chen KY, Manabe Y, Ward JL, Goodyear LJ, Tong Q. 2009. Diet and exercise signals regulate SIRT3 and activate AMPK and PGC-1alpha in skeletal muscle. *Aging* **1**:771–783. DOI: https://doi.org/10.18632/aging.100075, PMID: 20157566

Qin X, Qiu C, Zhao L. 2014. Lysophosphatidylcholine perpetuates macrophage polarization toward classically activated phenotype in inflammation. *Cellular Immunology* **289**:185–190. DOI: https://doi.org/10.1016/j.cellimm.2014.04.010, PMID: 24841857

Rawat M, Srivastava A, Johri S, Gupta I, Karmodiya K. 2021. Single-cell RNA sequencing reveals cellular heterogeneity and stage transition under temperature stress in synchronized *Plasmodium falciparum* cells. *Microbiology Spectrum* **9**:e0000821. DOI: https://doi.org/10.1128/Spectrum.00008-21, PMID: 34232098

Recker M, Nee S, Bull PC, Kinyanjui S, Marsh K, Newbold C, Gupta S. 2004. Transient cross-reactive immune responses can orchestrate antigenic variation in malaria. *Nature* **429**:555–558. DOI: https://doi.org/10.1038/nature02486, PMID: 15175751

Reis A, Rudnitskaya A, Blackburn GJ, Fauzi NM, Pitt AR, Spickett CM. 2013. A comparison of five lipid extraction solvent systems for lipidomic studies of human LDL. *Journal of Lipid Research* **54**:1812–1824. DOI: https://doi.org/10.1194/jlr.M034330, PMID: 23670529

Rono MK, Nyonda MA, Simam JJ, Ngoi JM, Mok S, Kortok MM, Abdullah AS, Elfaki MM, Waitumbi JN, El-Hassan IM, Marsh K, Bozdech Z, Mackinnon MJ. 2018. Adaptation of *Plasmodium falciparum* to its transmission environment. *Nature Ecology & Evolution* **2**:377–387. DOI: https://doi.org/10.1038/s41559-017-0419-9, PMID: 29255304

Rottmann M, Lavstsen T, Mugasa JP, Kaestli M, Jensen ATR, Müller D, Theander T, Beck HP. 2006. Differential expression of var gene groups is associated with morbidity caused by *Plasmodium falciparum* infection in tanzanian children. *Infection and Immunity* **74**:3904–3911. DOI: https://doi.org/10.1128/IAI.02073-05, PMID: 16790763

Rowe JA, Claessens A, Corrigan RA, Arman M. 2009. Adhesion of *Plasmodium falciparum*-infected erythrocytes to human cells: molecular mechanisms and therapeutic implications. *Expert Reviews in Molecular Medicine* **11**:e16. DOI: https://doi.org/10.1017/S1462399409001082, PMID: 19467172

Salanti A, Staalsoe T, Lavstsen T, Jensen ATR, Sowa MPK, Arnot DE, Hviid L, Theander TG. 2003. Selective upregulation of a single distinctly structured var gene in chondroitin sulphate A-adhering *Plasmodium falciparum* involved in pregnancy-associated malaria. *Molecular Microbiology* **49**:179–191. DOI: https://doi.org/10.1046/j.1365-2958.2003.03570.x, PMID: 12823820

Scheltema RA, Jankevics A, Jansen RC, Swertz MA, Breitling R. 2011. PeakML/mzmatch: a file format, java library, R library, and tool-chain for mass spectrometry data analysis. *Analytical Chemistry* **83**:2786–2793. DOI: https://doi.org/10.1021/ac2000994, PMID: 21401061

Scherf A, Lopez-Rubio JJ, Riviere L. 2008. Antigenic variation in *Plasmodium falciparum*. *Annual Review of Microbiology* **62**:445–470. DOI: https://doi.org/10.1146/annurev.micro.61.080706.093134, PMID: 18785843

Shapouri-Moghaddam A, Mohammadian S, Vazini H, Taghadosi M, Esmaeili SA, Mardani F, Seifi B, Mohammadi A, Afshari JT, Sahebkar A. 2018. Macrophage plasticity, polarization, and function in health and disease. *Journal of Cellular Physiology* **233**:6425–6440. DOI: https://doi.org/10.1002/jcp.26429, PMID: 29319160

Silamut K, Phu NH, Whitty C, Turner GD, Louwrier K, Mai NT, Simpson JA, Hien TT, White NJ. 1999. A quantitative analysis of the microvascular sequestration of malaria parasites in the human brain. *The American Journal of Pathology* **155**:395–410. DOI: https://doi.org/10.1016/S0002-9440(10)65136-X, PMID: 10433933

Sinha A, Hughes KR, Modrzynska KK, Otto TD, Pfander C, Dickens NJ, Religa AA, Bushell E, Graham AL, Cameron R, Kafsack BFC, Williams AE, Llinas M, Berriman M, Billker O, Waters AP. 2014. A cascade of DNA-binding proteins for sexual commitment and development in plasmodium. *Nature* **507**:253–257. DOI: https://doi.org/10.1038/nature12970, PMID: 24572359

Smith JD, Chitnis CE, Craig AG, Roberts DJ, Hudson-Taylor DE, Peterson DS, Pinches R, Newbold CI, Miller LH. 1995. Switches in expression of *Plasmodium falciparum* var genes correlate with changes in antigenic and cytoadherent phenotypes of infected erythrocytes. *Cell* **82**:101–110. DOI: https://doi.org/10.1016/0092-8674(95)90056-x, PMID: 7606775

Smith CA, Want EJ, O'Maille G, Abagyan R, Siuzdak G. 2006. XCMS: processing mass spectrometry data for metabolite profiling using nonlinear peak alignment, matching, and identification. *Analytical Chemistry* **78**:779–787. DOI: https://doi.org/10.1021/ac051437y, PMID: 16448051

Sorci G, Léchenault-Bergerot C, Faivre B. 2021. Age reduces resistance and tolerance in malaria-infected mice. *Infection, Genetics and Evolution* **88**:104698. DOI: https://doi.org/10.1016/j.meegid.2020.104698, PMID: 33370596

Su XZ, Heatwole VM, Wertheimer SP, Guinet F, Herrfeldt JA, Peterson DS, Ravetch JA, Wellems TE. 1995. The large diverse gene family var encodes proteins involved in cytoadherence and antigenic variation of *Plasmodium falciparum*-infected erythrocytes. *Cell* **82**:89–100. DOI: https://doi.org/10.1016/0092-8674(95)90055-1, PMID: 7606788

Tan JL, Lash B, Karami R, Nayer B, Lu YZ, Piotto C, Julier Z, Martino MM. 2021. Restoration of the healing microenvironment in diabetic wounds with matrix-binding IL-1 receptor antagonist. *Communications Biology* **4**:422. DOI: https://doi.org/10.1038/s42003-021-01913-9, PMID: 33772102

Taylor TE, Fu WJ, Carr RA, Whitten RO, Mueller JS, Fosiko NG, Lewallen S, Liomba NG, Molyneux ME. 2004. Differentiating the pathologies of cerebral malaria by postmortem parasite counts. *Nature Medicine* **10**:143–145. DOI: https://doi.org/10.1038/nm986, PMID: 14745442

Tonkin CJ, Carret CK, Duraisingh MT, Voss TS, Ralph SA, Hommel M, Duffy MF, Silva L da, Scherf A, Ivens A, Speed TP, Beeson JG, Cowman AF. 2009. Sir2 paralogues cooperate to regulate virulence genes and antigenic variation in *Plasmodium falciparum*. *PLOS Biology* **7**:e84. DOI: https://doi.org/10.1371/journal.pbio.1000084, PMID: 19402747

Turner L, Lavstsen T, Berger SS, Wang CW, Petersen JEV, Avril M, Brazier AJ, Freeth J, Jespersen JS, Nielsen MA, Magistrado P, Lusingu J, Smith JD, Higgins MK, Theander TG. 2013. Severe malaria is associated with parasite binding to endothelial protein C receptor. *Nature* **498**:502–505. DOI: https://doi.org/10.1038/nature12216, PMID: 23739325

Usui M, Prajapati SK, Ayanful-Torgby R, Acquah FK, Cudjoe E, Kakaney C, Amponsah JA, Obboh EK, Reddy DK, Barbeau MC, Simons LM, Czesny B, Raiciulescu S, Olsen C, Abuaku BK, Amoah LE, Williamson KC. 2019. Publisher correction: *Plasmodium falciparum* sexual differentiation in malaria patients is associated with host factors and GDV1-dependent genes. *Nature Communications* **10**:2740. DOI: https://doi.org/10.1038/s41467-019-10805-w, PMID: 31227704

Vasquez MC, Beam M, Blackwell S, Zuzow MJ, Tomanek L. 2017. Sirtuins regulate proteomic responses near thermal tolerance limits in the blue mussels mytilus galloprovincialis and *Mytilus trossulus*. *The Journal of Experimental Biology* **220**:4515–4534. DOI: https://doi.org/10.1242/jeb.160325, PMID: 29025872

Weiss ES, Girard-Guyonvarc'h C, Holzinger D, de Jesus AA, Tariq Z, Picarsic J, Schiffrin EJ, Foell D, Grom AA, Ammann S, Ehl S, Hoshino T, Goldbach-Mansky R, Gabay C, Canna SW. 2018. Interleukin-18 diagnostically distinguishes and pathogenically promotes human and murine macrophage activation syndrome. *Blood* **131**:1442–1455. DOI: https://doi.org/10.1182/blood-2017-12-820852, PMID: 29326099

White NJ. 2018. Anaemia and malaria. *Malaria Journal* **17**:371. DOI: https://doi.org/10.1186/s12936-018-2509-9, PMID: 30340592

WHO. 2022. World malaria Report. WHO.

Williams JL. 1999. Stimulation of *Plasmodium falciparum* gametocytogenesis by conditioned medium from parasite cultures. *The American Journal of Tropical Medicine and Hygiene* **60**:7–13. DOI: https://doi.org/10.4269/ajtmh.1999.60.7, PMID: 9988315

Zheng L, T'Kind R, Decuypere S, von Freyend SJ, Coombs GH, Watson DG. 2010. Profiling of lipids in leishmania donovani using hydrophilic interaction chromatography in combination with fourier transform mass spectrometry. *Rapid Communications in Mass Spectrometry* **24**:2074–2082. DOI: https://doi.org/10.1002/rcm.4618, PMID: 20552712

Zhu AY, Zhou Y, Khan S, Deitsch KW, Hao Q, Lin H. 2012. *Plasmodium falciparum* sir2a preferentially hydrolyzes medium and long chain fatty acyl lysine. *ACS Chemical Biology* **7**:155–159. DOI: https://doi.org/10.1021/cb200230x, PMID: 21992006